Check for updates

Water Practice & Technology

IWA PUBLISHING

Assessing the impact of COVID-19 lockdowns on water quality in Anzali Wetland, Iran, using remote sensing data

Mohammad Reza Goodarzi [a,b,*], Amir Reza R. Niknam [c], Maryam Sabaghzadeh[c], Mohammad Hossein Mokhtari[d] and Majid Niazkar [e,f]

[a] Department of Civil Engineering, Faulty of Engineering, Ferdowsi University of Mashhad, Mashhad, Iran
[b] Department of Civil Engineering, Yazd University, Yazd, Iran
[c] Department of Civil Engineering, Water Resources Management Engineering, Yazd University, Yazd, Iran
[d] Faculty of Natural Resources, Yazd University, Yazd, Iran
[e] Euro-Mediterranean Center on Climate Change, Italy
[f] Ca'Foscari University of Venice, Italy
*Corresponding author. E-mail: goodarzimr@um.ac.ir; goodarzimr@yazd.ac.ir

MRG, 0000-0002-6296-2315; ARRN, 0000-0002-1526-9462; MN, 0000-0002-5022-1026

ABSTRACT

This study investigates temporal variations of two water quality indices, named turbidity and Chlorophyll-a (Chl-a), from 2016 to 2021 in the Anzali wetland. For this purpose, ground-based measurements were collected at four stations from 2016 to 2019, while Sentinel-2 images were utilized to predict Chl-a and turbidity from 2016 to 2021. To validate the forecasted results, remote sensing data for Chl-a and turbidity were compared to measurements. After the validation step, Chl-a and turbidity were predicted using remotely-sensed data for the first and fourth peaks of the COVID-19 pandemic, which coincide with the COVID-19 lockdowns in 2020 and 2021 in Iran, respectively. The results indicate 26% and 16% decreases in Chl-a and turbidity in the COVID-19 lockdown imposed in 2020, while it yielded to 1% decrease in turbidity and 21% increase in the Chl-a concentration in the COVID-19 lockdown applied in 2021, compared to the corresponding mean values measured from 2016 to 2019. In conclusion, the lockdown imposed in 2020, which turned out to be a much more restricted quarantine than the one applied in 2021, was found to be one of the primary reasons behind improving water quality indices of Anzali wetland in March and April of 2020.

Key words: chlorophyll-a, COVID-19 lockdowns, remote sensing, turbidity, water quality

HIGHLIGHTS

- This study investigates the lockdown's effects on the Anzali western wetland turbidity and Chl-a.
- In 2021, Chl-a concentration in wetland increased by 21% and turbidity decreased by 1%.
- Changes in turbidity and chlorophyll-a concentration are mainly related to human activities.

GRAPHICAL ABSTRACT
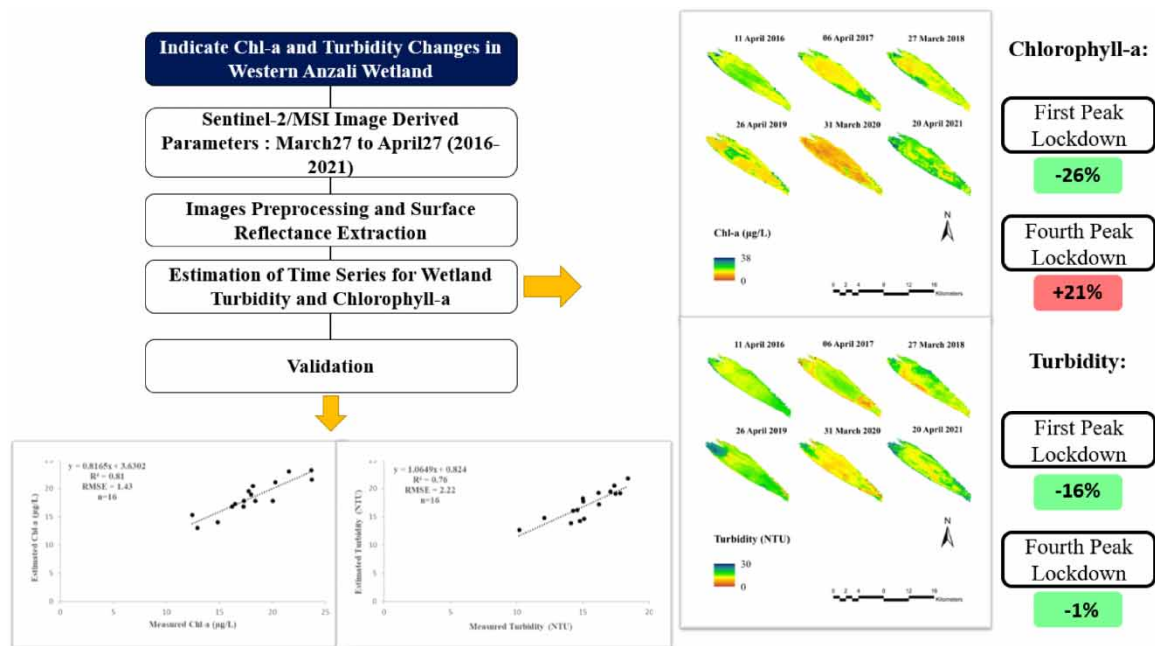
1. INTRODUCTION

The COVID-19 pandemic attempts to alter not only human lives but also environment and is a unique problem (Rahman *et al.* 2021). In the combat against the vigorous COVID-19 outbreak, lockdowns are counted as one of the most controlling measures (Niazkar *et al.* 2020). During partial and full quarantine, various high- and low-risk businesses may be shut down. Although the curfew period inevitably brings about financial disadvantages, it not only significantly reduces the number of positive COVID-19 cases but also pandemic offers a rare chance to examine the interplay between human activity and environmental changes (Venter *et al.* 2020; Xu *et al.* 2021). For instance, air quality is expected to improve as activities ceased, whereas wastewater discharge, which had a significant impact on the surrounding aquatic environment, may be reduced. Under the lockdown circumstances, it is vital to quantify influences that industrial activities and humans' actions had on different aspects of environment (Patel *et al.* 2020; Yunus *et al.* 2020). Water plays a crucial role as the primary resource for maintaining ecosystem stability, being indispensable for both human populations and natural environments (Niknam *et al.* 2024). Consequently, evaluating the quality of water is of paramount significance.

Several studies have reported mixed findings regarding the determinants and causing factors of COVID-19 to provide useful implications and to take control of the spread (e.g., Bhadra *et al.* 2021; Roy *et al.* 2021; Mansouri Daneshvar *et al.* 2022). Also, based on the literature, many studies have been carried out to delineate different environmental factors in the absence or reduction of humans' actions during the lockdown periods. For instance, Venter *et al.* (2020) surveyed air pollution x in 34 countries during the lockdown period due to COVID-19. They showed that the reduction of transportation and travel has decreased the rate of nitrogen dioxide emissions and the amount of airborne suspended matter by 60 and 31%, respectively. Furthermore, it is stipulated that the state of water pollution would improve in rivers and various watercourses with the cessation of not only industrial activities but also sewage discharge. Studies conducted on various rivers and lakes during the COVID-19 pandemic deduced the same result. For instance, Patel *et al.* (2020) investigated the Yamuna River in Delhi, which is known to be the most polluted river in India. They found that the water quality index (WQI) of nine stations was improved by 37% during the lockdown period. In addition, biochemical oxygen demand (BOD) and chemical oxygen demand (COD) reduced by 42.83 and 39.25%, respectively. Furthermore, the values of turbidity, total suspended solids (TSS), and the algae effect were calculated using Landsat-8 images, while they showed a significant reduction during the lockdown period.

The quality of water is affected by the type of land cover and land use in an area (Goodarzi *et al.* 2023). According to the literature review, most of research during the COVID-19 outbreak uses satellite imagery to assess water quality. One of the most significant advantages of using remote sensing imagery over ground-based data is its

broader coverage across the globe (Goodarzi et al. 2022a). For instance, Cherif et al. (2020) studied water temperature and quality at the west coast of Tangier, Morocco, using Sentinel-3 images at multiple points in April 2019 and 2020. Their results indicated a decrease in water temperature and an improvement in water quality during the lockdown. Their finding can be utilized to manage coastal activities. Aman et al. (2020) found that the amount of suspended matter in the water of the Sabarmati River in Ahmedabad, India, decreased approximately by 36.48% during the lockdown period and reached 16.79%. Moreover, air quality in Ahmedabad has been improved according to the Center for Air Pollution Control. In another study, Yunus et al. (2020) used Landsat-8 images to calculate suspended particulate matter (SPM) in Vembanad River, which is the longest freshwater river in India. It was observed that SPM decreased by 15.9% due to the decrease in tourism and industrial activities. To be more specific, the SPM rate decreased at 11 points out of 20 in April 2020. In addition, Niroumand-Jadidi et al. (2020) examined water properties and total suspended matter (TSM) in the Venice Lagoon during and before a lockdown. Their results showed a reduction of TSM and water turbidity during the lockdown period. Also, Avtar et al. (2020) compared chlorophyll-a (Chl-a) using Landsat-8 and Sentinel-2 images in Lake Vembanad and Wuhan between the pre-lockdown and during lockdown. The results demonstrated an increase in Wuhan, while there were no significant changes in Vembanad. Muduli et al. (2021) used Sentinel-2 satellite imagery to analyze water turbidity before and during a lockdown at seven specific points on the Ganges River in India. It was found that water turbidity reduced by 55%, which is due to reduced industrial activity, urban pollution, and hotels and domestic sewage. Also, it was indicated that the amounts of dissolved oxygen (DO), BOD, and NO_3 were decreased. Similarly, Tokatlı & Varol (2021) calculated the amount of physical and chemical variables and heavy metals at 25 stations on the Ergene River Basin in Turkey. It revealed a decrease in the aforementioned parameters during the lockdown period. However, there was no significant decrease in BOD, COD, TSS, EC, Mn, and turbidity, which could be due to the increased domestic sewage. Khan et al. (2021) computed that the DO rate during and after the lockdown period in the Gomati River in India were 69 and 79%, respectively. Also, the BOD rates during the lockdown period and after the lockdown period were 69 and 75%, respectively, which indicates a decrease in the rate of these parameters during the lockdown period. Najah et al. (2021) examined the WQI of Lake Putrajaya in Malaysia and concluded that it increased from 24% in February 2020 to 94% during the lockdown period. Their results showed that NH3N and COD factors play a key role in determining the WQI class, whereas pH, DO, and TSS are less effective. Xu et al. (2021) studied a series of time series of Landsat 5 and 8 satellite images taken from November 2019 to April 2020 on the China Min River. Their investigation resulted in a 48% reduction in TSS concentration during this period due to the reduced industrial, urban, and shipping activities on the corresponding river.

Ritchie et al. (2003) examined water quality parameters such as temperature, chlorophyll, and suspended particles in water using satellite images. They concluded that the use of satellite data, global positioning system, and geographic information system is versatile to expand management programs for natural resources. Gholizadeh et al. (2016) tabulated various specifications of airborne sensors to be used as a guide. They also assessed the most common sensors in evaluating and calculating 11 water quality parameters, such as Chl-a, TSS, water temperature, DO, BOD, and COD.

The first case of COVID-19 was observed in Iran in February 2020. The Iranian Ministry of Health quickly intervened and tried to control the spreading of the disease by imposing restrictions and closing schools, universities, and shopping malls. However, it spread rapidly across the country. In March 2020, more restrictions were imposed. In this regard, people were asked to follow new regulations surrounding social distance in their daily activities and stay home, if possible. In addition, all industrial activities, trains, planes, and travel were stopped. On 10 March 2020 and 9 April 202, a full lockdown was imposed in Iran. As a result, factories and tourist sites were closed, industrial production was stopped, and agricultural activities were minimized.

The current study aims to investigate the effects of the lockdown imposed in Iran on two water quality parameters (turbidity and Chl-a) of the western part of Anzali Wetland. The investigation of the water quality of Anzali Wetland is very important, particularly due to its extensive impacts on the environment and the regional economy. Anzali Wetland is one of the largest natural wetlands in Iran and is highly valuable for preserving biodiversity, water regulation, water resource provision, and natural resource conservation (Fallah & Zamani-Ahmadmahmoodi 2017). This lagoon, as a sensitive ecosystem, requires protection and care. Assessing water quality can help us address environmental issues such as water pollution, depletion of water resources, and destruction of natural habitats. For this purpose, ground-based data and remote sensing techniques were used to accounting for various influential factors including natural and human factors. The data gathered in this

study were compared with each other to quantify variations of water quality parameters in the lockdown periods of 2020 and 2021. The results help not only to understand the factors affecting changes in water quality but also to identify the impact of human activities on the wetland system.

2. MATERIALS AND METHODS

2.1. Study area and datasets

2.1.1. Study area

Anzali Wetland is one of the international natural wetlands and is located in Guilan province, Iran. The approximate area of the wetland catchment is 3,740 km^2, of which about 2,000 km^2 is plains and other mountainous areas. Moreover, it is in the geographical range of 36 degrees and 55 min to 37 degrees and 32 min north and also 48 degrees and 45 min to 49 degrees and 42 min east. The average length of the wetland from east to west is about 30 km, while its average width from north to south is about 3 km. Furthermore, the average long-term annual rainfall is 1,300 mm with a considerable spatial and temporal variation, while 40% of rainfall is commonly limited to the autumn season (September to January) (Aghsaei *et al.* 2020).

Basically, Anzali Wetland is divided into four main parts (east, west, central, and Siah Kashim), while the central part is connected to the Caspian Sea. The study region is the western part of the wetland, which is shown in Figure 1. The western part is similar to a small lake due to the great stillness of water and deep water depth. This part is remarkably important for native residents who primarily exploit the region for fishing (Hosseinjani *et al.* 2019).
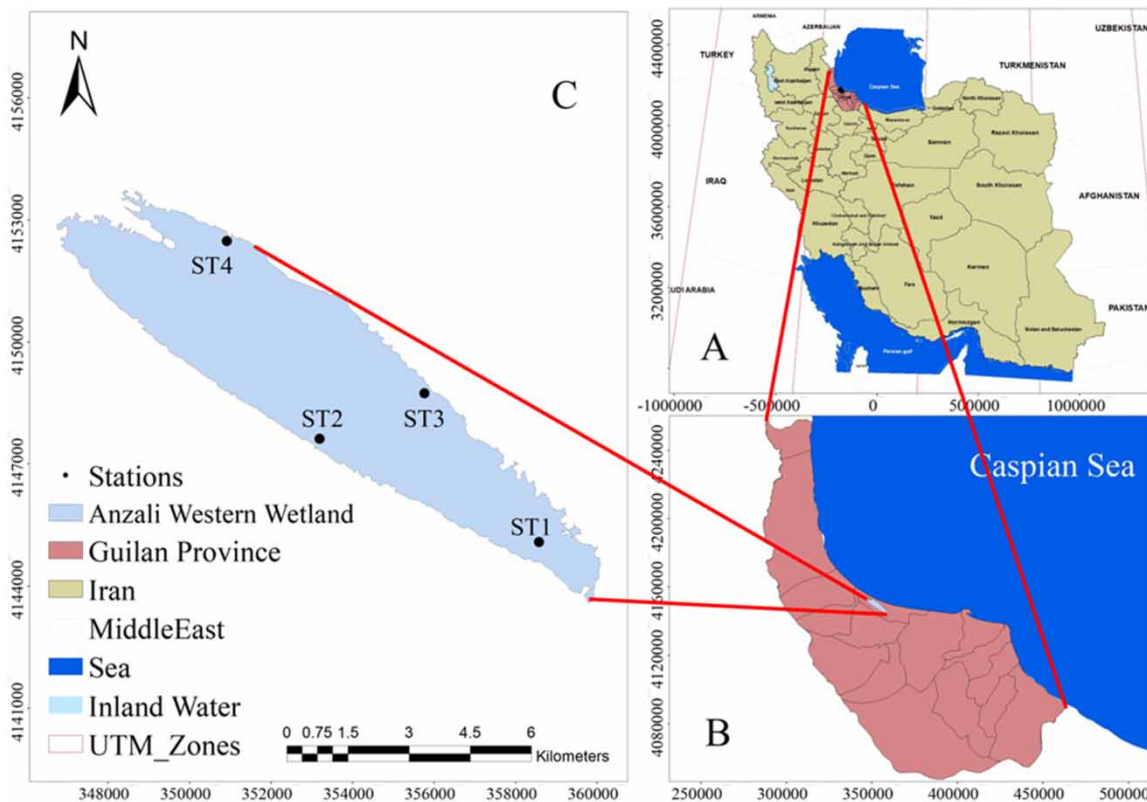
Figure 1 | The study area (c) in Guilan province (b).

2.1.2. In situ measurement

In this study, the focus is on two water quality parameters, namely, turbidity and Chl-a. In this regard, the first part of the data, which were measured from 2016 to 2019, were prepared by the Regional Water Administration of Guilan Province and reliable sources (ALabdeh *et al.* 2020). The location of the sampling stations is depicted in Figure 1(c), and their coordinates are presented in Table 1. Generally, the standard units for turbidity and

Table 1 | Geographical location of four sampling stations in the western part of Anzali Wetland

Sampling stations	Geographical location	
	Longitude	Latitude
ST1	49°24′4.65″E	37°26′30.4″N
ST2	49°20′23.96″E	37°27′49.7″N
ST3	49°22′7.92″E	37°28′27.4″N
ST4	49°18′47.83″E	37°30′26. 9″N

Chl-a are nephelometric turbidity unit (NTU) and micrograms per liter, respectively. In addition, the second part of the data, which belong to the years of 2020 and 2021, was not directly measured due to the lockdown restrictions, which include non-issuance of licenses for vehicle traffic between cities. Thus, there is a lack of field measurements during the lockdown period.

2.1.3. Satellite images

In areas where investigating features is difficult or where data collection stations are absent, satellite imagery can be of significant assistance (Goodarzi *et al.* 2022b). The Sentinel-2/MSI satellite imagery was used for obtaining the second part of the data in this study. Sentinel 2 satellites have multispectral imagery and provide the right dataset to monitor the quality of a water body (Buma & Lee 2020). Basically, it is an Earth observation project developed by the European Space Agency as a part of the Copernicus program. The imaging sensor mounted on this satellite operates in the visible, near-infrared (NIR), and infrared spectral ranges. Furthermore, it has 13 imaging bands with a spatial resolution of 20, 10, and 60 m and an imaging width of 290 km (Garg *et al.* 2020). For better clarification, the specifications of this sensor are presented in Table 2. The main objectives of Sentinel 2 are not only to improve Earth observation missions but also to support remote sensing services, such as forest monitoring, land cover change monitoring, and natural disaster management. A total of six high-quality and free-cloud satellite images of the study region were selected in this study. The selected images of the Sentinel-2/MSI satellite were downloaded from the US Geological Survey (www.earthexplorer.usgs.gov) (Table 2).

2.1.4. Meteorological data

Meteorological data and information for the study area, such as temperature and rainfall and wind speed, were gathered from the website of the Meteorological Organization of Iran (www.irimo.ir/eng/index.php) and the World Weather online website (www.worldweatheronline.com) on a daily basis and monthly for March and April from 2016 to 2021.

2.2. Images preprocessing

The current study utilized ENVI 5.3.1 software for satellite images preprocessing. The QUick Atmospheric Correction (QUAC) algorithm was also employed to correct the visible bands of Sentinel-2 (Mahdavifard *et al.* 2020). The input of the QUAC algorithm can be both radiance and Top of Atmosphere (TOA) reflectance (the data used by Sentinel in this study were TOA data). The output of this image algorithm is surface reflectance (SR) with pixel values of the Earth.

2.3. Estimation of Chl-a

Estimating the amount of Chl-a by using remote sensing methods is one of the most widely used efforts in evaluating water quality. There are a variety of algorithms for calculating Chl-a, which may include the use of single bands, rationing, or indicators, such as Normalized Difference Vegetation Index (NDVI). In this study, the Chl-a data were extracted from satellite images, and its map was prepared from 2016 to 2021 (March 27–April 27). Prior to the implementation of the Chl-a model, pixels that included sunlight and regions other than the water body were covered using the SR threshold short-wave infrared band. In this regard, Equations (1) and (2) presented the equations proposed by Mishra & Mishra (2012) to obtain Chl-a with a high accuracy (determination coefficient (R^2) = 0.95; $p < 0.0001$; range = 1–60 μg/L; root-mean-square error (RMSE) = 2 μg/L) (Mishra & Mishra 2012). This relationship has been widely used by numerous remote sensing studies (Muduli *et al.* 2021). As shown in Equations (1) and (2), the normalized index of Chl-a difference (NDCI) is first obtained. To be more

Table 2 | Sentinel-2 MSI images of the Anzali western wetland used in this study

Name	Bands	Central wavelengths (nm)	Resolution (m)	Revisit period	Swath width	Date of image acquisition	Product ID
Sentinel 2/MSI	B1	443	10–20–60	5 days	290 km	2016-04-11	S2A_OPER_PRD_MSIL1C_PDMC_20160412T231157_R049_V20160411T073735_20160411T073735.SAFE
	B2	490				2017-04-06	S2A_MSIL1C_20170406T072611_N0204_R049_T39SUB_20170406T073122.SAFE
	B3	560				2018-03-27	S2B_MSIL1C_20180327T072609_N0206_R049_T39SUB_20180327T112210.SAFE
	B4	665				2019-04-26	S2A_MSIL1C_20190426T072621_N0207_R049_T39SUB_20190426T093248.SAFE
	B5	705				2020-03-31	S2A_MSIL1C_20200331T072611_N0209_R049_T39SUB_20200331T093103.SAFE
	B6	740				2021-04-20	S2B_MSIL1C_20210420T072609_N0300_R049_T39SUB_20210420T082640.SAFE
	B7	783					
	B8	842					
	B8a	865					
	B9	945					
	B10	1,375					
	B11	1,610					
	B12	2,190					

precise, Equation (1) gives NDCI from the Sentinel 2 outputs:

$$NDCI = \frac{\rho(705) - \rho(665)}{\rho(705) + \rho(665)} \tag{1}$$

$$Chl - a = 14.039 + 86.115 \times NDCI + 194.325 \times NDCI^2 \tag{2}$$

where ρ is the SR, which are calculated at 705 and 665 nm of the Sentinel 2-MSI bands.

2.4. Estimation of turbidity

Turbidity is a measure of the transparency of a liquid. It is a visual property of water and measured by the amount of light emitted by the material irradiated into the water. Water turbidity may be caused by the presence of planktons or microscopic organisms, suspended solids, such as clay and sludge, organic acids, dyes, and finely divided organic matter (Nas *et al.* 2010). Several studies have extensively used visible and NIR bands to model turbidity in lakes and reservoirs (Wang *et al.* 2006; Nas *et al.* 2010; Hicks *et al.* 2013; Baughman *et al.* 2015; Masocha *et al.* 2018; Martins *et al.* 2019; Abirhire *et al.* 2020).

Basically, the turbidity is calculated by preprocessing the satellite images, which is applied as a mask on the study region. The method considered in this study involves the model developed by Abirhire *et al.* (2020). It uses green, red, and NIR bands. This model is shown in Equation (3) and was selected because of its acceptable precision ($R^2 = 0.91$, $n = 37$, $P \leq 0.001$). It was originally presented for Landsat 8/OLI satellite (Abirhire *et al.* 2020). However, equivalent bands were used for Sentinel 2/MSI in this study.

$$Turbidity = -1.3790 + 55.3844 \times N + 6.4725 \times R/G - 5.6511 \times N/G \tag{3}$$

where G denotes green band, R is red band, and N is NIR2 (B8a).

2.5. Statistical metrics

Different statistical metrics have been employed for model assessment, each providing a distinct approach to quantify the disparity between observed and estimated values. Among the three error evaluation metrics examined are the correlation coefficient (R), the RMSE, and the mean absolute error (MAE), with their respective formulas provided below:

$$R = \frac{\sum_{1}^{n} (WQI_O - \overline{WQI_O})(WQI_F - \overline{WQI_F})}{\sqrt{\sum_{1}^{n} (WQI_O - \overline{WQI_O})^2 . \sum_{1}^{n} (WQI_F - \overline{WQI_F})^2}} \tag{4}$$

$$RMSE = \sqrt{\frac{\sum_{1}^{n} (WQI_F - WQI_O)^2}{N}} \tag{5}$$

$$MAE = \frac{\sum_{1}^{n} |WQI_F - WQI_O|}{N} \tag{6}$$

3. RESULTS

3.1. Estimating Chl-a and turbidity

The Chl-a concentration was investigated in the western part of Anzali Wetland using ground-based and remotely sensed data. Figure 2 illustrates the temporal variability of Chl-a concentration in March and April from 2016 to 2021. As shown, six images overall are presented in time series. According to the images depicted in Figure 2, it can be interpreted that the concentration of Chl-a decreased during the first lockdown, which was in 2020. To be more precise, the average value of the Chl-a concentration, which was 16.23 in 2019, reached 12.8 µg/L in 2020. This decrease in the Chl-a concentration can also be seen in the satellite images. However, the concentration of
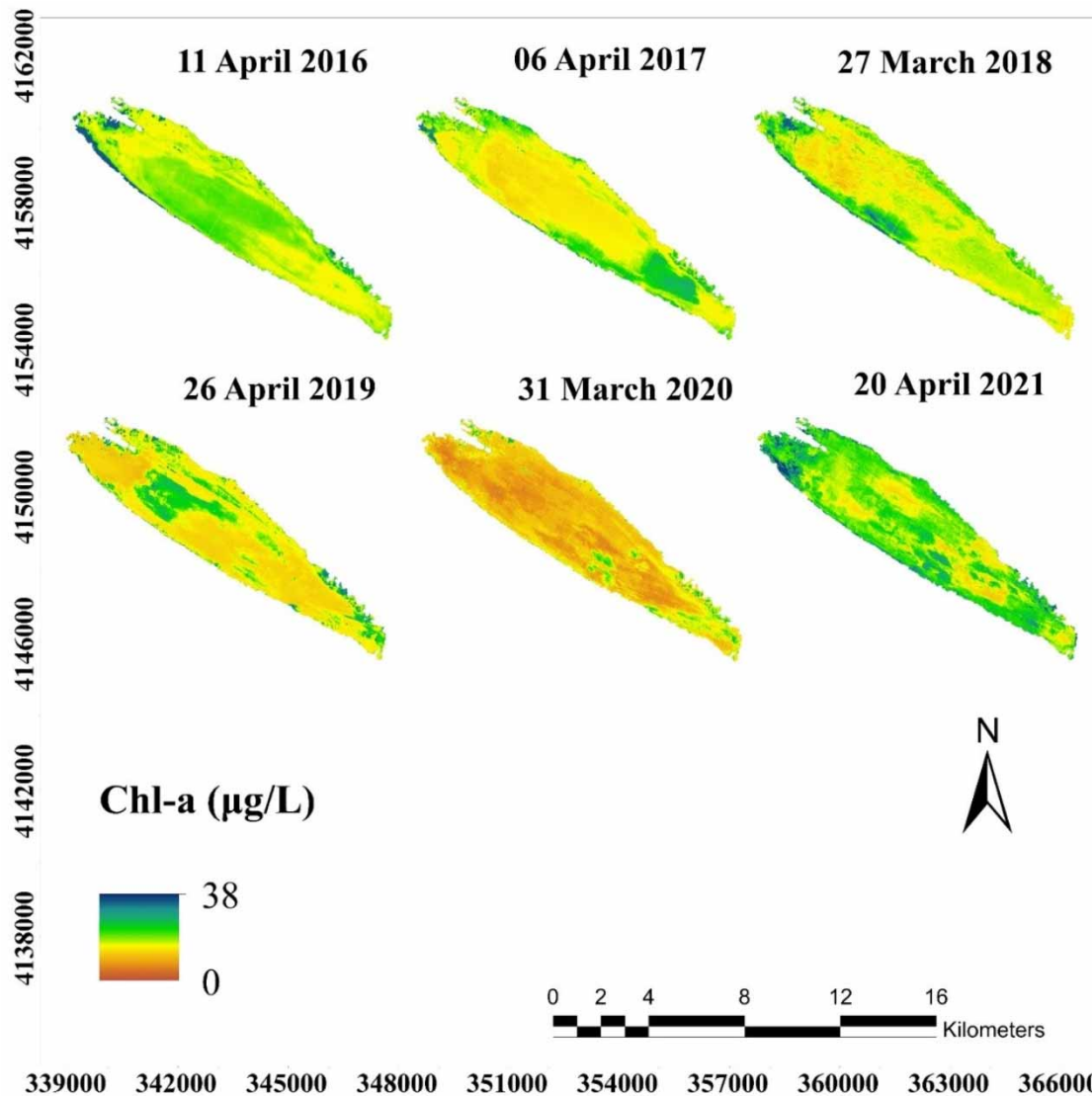
Figure 2 | Chl-a concentrations estimated for the western part of Anzali Wetland from March 27 to April 27 (2016–2021).

Chl-a increased to 20.9 µg/L during the lockdown corresponds to the fourth peak of the COVID-19 pandemic that occurred in 2021.

By using the model presented by Abirhire *et al.* (2020), the turbidity of the study area was achieved from the Sentinel-2 images in the period of 2016 to 2021 (March 27–April 27). The corresponding images can be observed in Figure 3. As shown, the results obtained in the first lockdown visually demonstrate a trend almost identical to that obtained for the Chl-a concentration. There was a significant reduction in the turbidity of the west part water in 2020. To be more specific, an average turbidity of 18.78 NTU in 2019 was reduced to 14.84 in 2020. According to Figures 2 and 3, water turbidity levels in April 2021 have increased compared to the previous year, and the central and southeastern parts of the lagoon have higher turbidity levels compared to 2020.

3.2. Validation of Chl-a and turbidity predictions

Previous studies calculated the correlation between Chl-a model (Mishra & Mishra 2012) and the turbidity model (Abirhire *et al.* 2020) with the corresponding field data. In this study, the turbidity value and Chl-a of the study area are compared in Figure 4 with 16 field-measured data obtained to ensure the accuracy of the estimation results. The field data were gathered from four stations between March 27 and April 27 (2016–2019). According to Figure 4, the results indicate a significant relationship between the field-measured values with the ones estimated by Mishra and Mishra's model (2012) ($R^2 = 0.81$; $p < 0.001$; RMSE = 1.43 µg/L) and Abirhire *et al.*'s
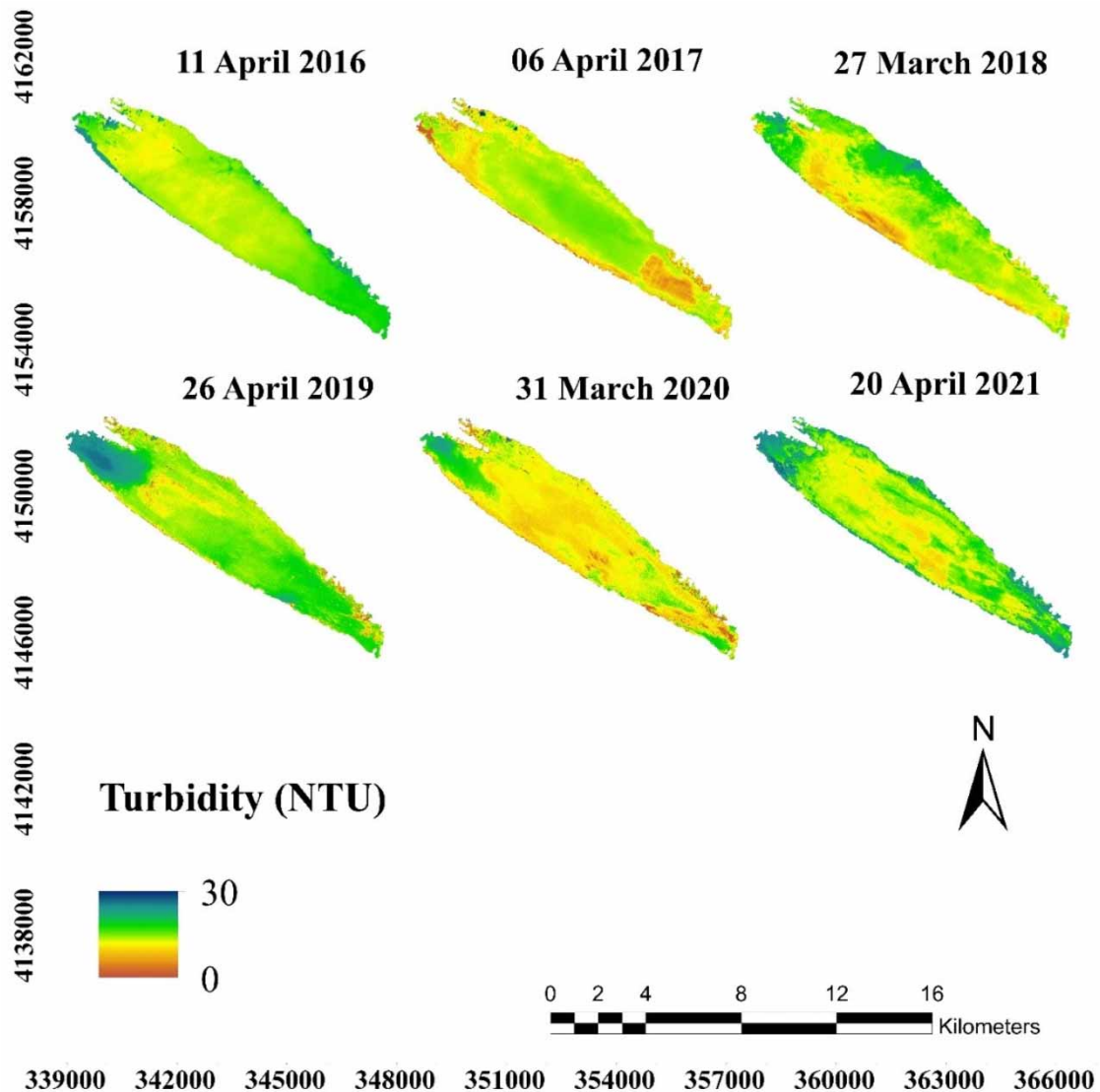
Figure 3 | Turbidity estimated for the western part of Anzali Wetland from March 27 to April 27 (2016–2021).

model (2020) ($R^2 = 0.76$; $p < 0.001$; RMSE $= 2.22$ NTU). In addition, Table 3 displays the values of all three statistical metrics. The results indicate that the parameter estimations have been conducted with acceptable accuracy. Since the predicted values of Chl-a and turbidity are accepted in the validation step, the predicted values are compared with the average Chl-a concentration and turbidity in Table 4. This comparison is conducted between the measured and estimated values from March 27 to April 27 (from 2016 to 2021). Also, Table 4 presents the percentage decrease in 2020 and 2021 from the average of the previous years.

3.3. Factors affecting turbidity and Chl-a

The climatic conditions of the study region were evaluated using meteorological data from the Meteorological Organization of Iran and the world weather website (www.worldweatheronline.com). This assessment was conducted to determine conditions, e.g., rain and wind, affecting turbidity and conditions, e.g., temperature, influencing Chl-a. For this purpose, Figure 5 presents time–series analysis of air temperature, rainfall, and wind speed. As shown, the average temperature in March and April 2020 did not change much compared to the previous years. However, the temperature increases by 5 °C in 2021. In addition, a significant decrease (10 mm) in rainfall was observed in 2021. The wind speed, the effect of wind force on the regeneration of some water components (algae and sediments), and their effect on water turbidity were also studied in previous studies (Penning *et al.* 2013; Xing *et al.* 2018; Sun *et al.* 2021). Based on Figure 5(c), the average wind speed from 2016 to 2021 was close to 8 km/h with an almost constant trend during the 6 years in question.
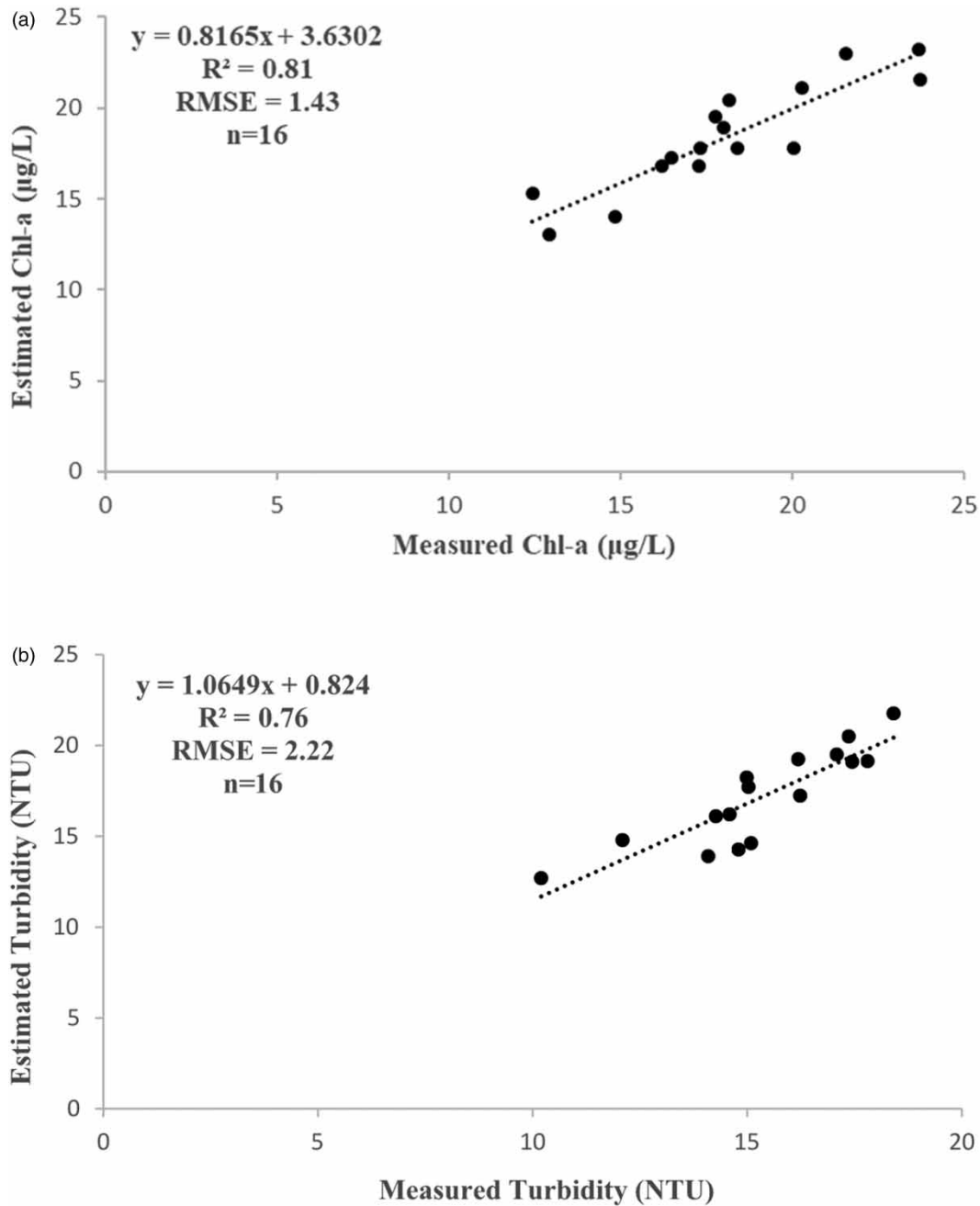
Figure 4 | Relationships between the estimated and field measured of (a) Chl-a concentration, (b) turbidity; from 2016 to 2019 (March 27 to April 27).

Table 3 | Results of statistical metrics

Parameter	R^2	RMSE	MAE
Chl-a	81	1.43	1.18
Turbidity	76	2.22	1.97

Another factor that may play a leading role in reducing Chl-a concentrations and turbidity is the decreased human activities. Nitrogen and phosphorus are essential elements for plants and living organisms. However, the entry of phosphorus and nitrogen from agricultural lands and completely untreated urban and industrial effluents into water can be one of the most important sources threatening water quality. Due to the COVID-19

Table 4 | The average concentration of Chl-a and turbidity from March 27 to April 27 (2016–2021) and the percentage decrease in 2020 and 2021 from the average of the previous years

Sampling point	Mean					Mean (% decrease)			
	2016	2017	2018	2019	Average of 2016–2019	2020		2021	
Chl-a (μg/L)	18.34	17.04	17.53	16.23	17.285	12.82	(−**26%**)	20.9	(**21%**)
Turbidity (NTU)	17.9	16.55	17.22	18.78	17.6125	14.84	(−**16%**)	17.38	(−**1%**)

lockdowns, human activities such as agriculture and factories were shut down. As a result, less nitrogen and phosphorus were entered into the wetland through sewage and runoff from agricultural lands. For this impact assessment, the temporal variations of Chl-a and turbidity from 2016 to 2021 are plotted in Figure 6. As shown, it is obvious that both Chl-a and turbidity reduced during the COVID-19 lockdowns, particularly during the first peak in 2020.

Figure 7 depicts the daily number of positive and death cases due to COVID-19 in March and April of 2020 and 2021. The corresponding data were adopted from a reliable source. As shown, a decrease in the number of positive and death cases of COVID-19 in 2020 after the first quarantine, whereas a significant increase in casualties and confirmed cases is observed in the fourth peak in comparison with the first one.

In addition to the factors mentioned in this study, factors such as the concentration of nutrients (nitrogen and phosphorus) also affect the amount of turbidity and Chl-a. However, for two reasons, the effects of these parameters were not directly considered in this study and were considered in the form of a possible decrease in wastewater output during the quarantine period: (1) Due to traffic restrictions due to the COVID-19 epidemic, it was not possible to sample phosphorus and nitrogen parameters on site. (2) The concentration of phosphorus and nitrogen parameters cannot be accurately calculated everywhere through remote sensing.
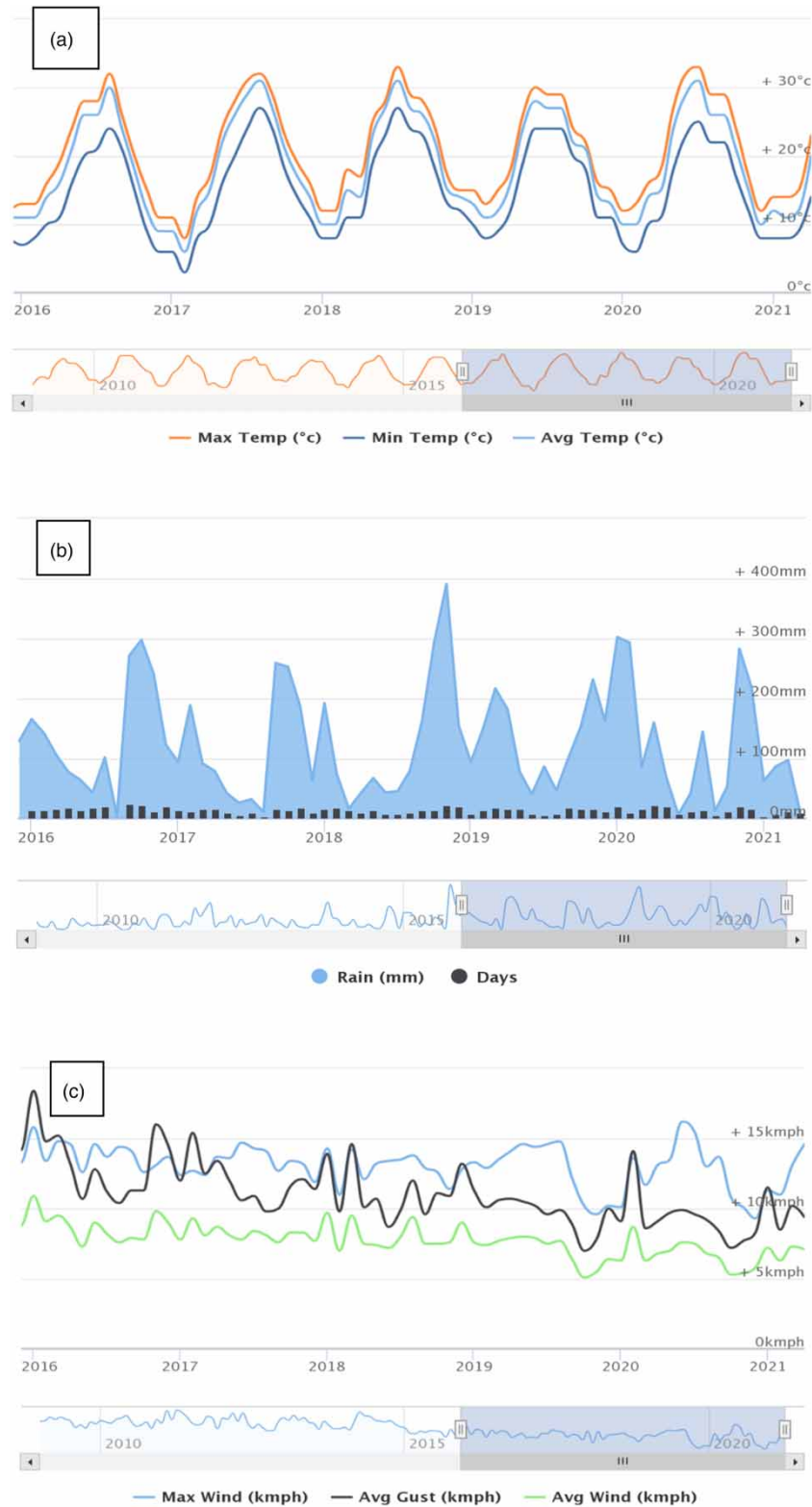
The lockdown restrictions and human activity reductions imposed during the 2020 and 2021 periods varied depending on the severity of the COVID-19 situation in different regions and countries. Here are some general trends:

2020:

1. *Strict lockdowns*: Many countries implemented strict lockdown measures, including stay-at-home orders, closure of non-essential businesses, and restrictions on movement.
2. *Reduced travel*: Travel restrictions were widespread, with many countries closing their borders to non-essential travel. This led to a significant reduction in domestic and international travel, including flights, trains, and public transportation.
3. *Remote work and education*: To minimize the spread of the virus, businesses and schools transitioned to remote work and online learning wherever possible. This led to a decrease in commuting and physical presence in workplaces and educational institutions.
4. *Decreased economic activity*: The closure of businesses and reduced consumer spending resulted in a decline in economic activity, leading to financial hardships for many individuals and businesses.
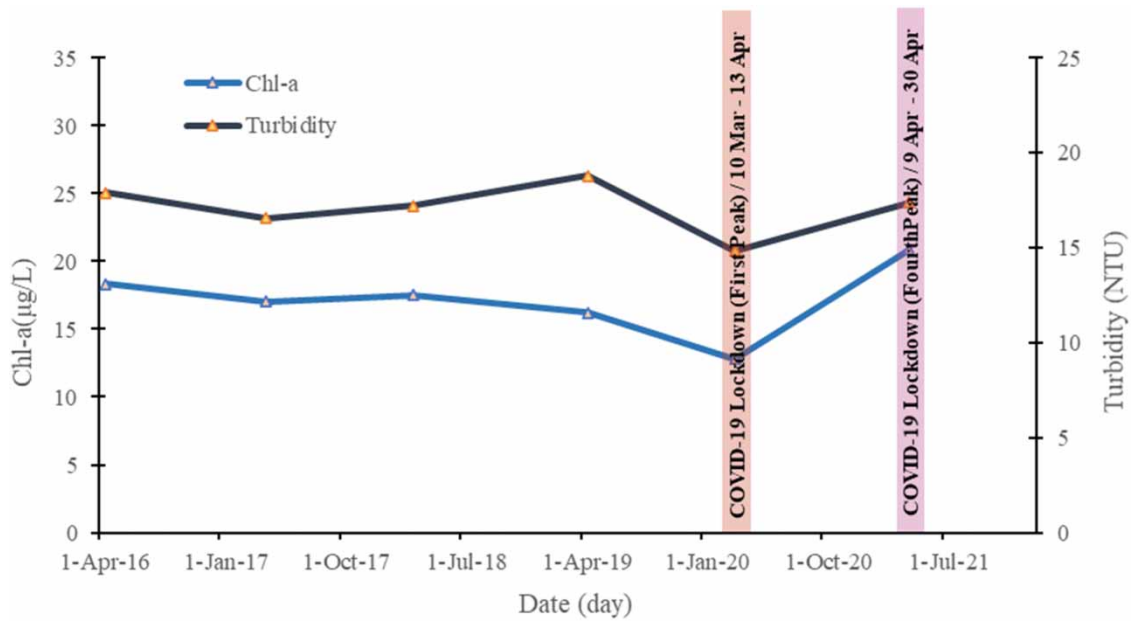
2021:

1. *Varied restrictions*: As vaccination efforts ramped up and some countries managed to control the spread of the virus, lockdown restrictions became more targeted and varied. Some regions experienced phased re-openings, while others maintained stricter measures.
2. *Continued travel restrictions*: While some travel restrictions were eased as vaccination rates increased, international travel remained limited in many places. Quarantine requirements and testing protocols were often in the place for travellers.
3. *Hybrid work and education*: Many organizations adopted hybrid work models, allowing employees to work both remotely and in-person. Similarly, educational institutions implemented hybrid learning approaches, combining online and in-person instruction.
4. *Economic recovery efforts*: Governments and businesses focused on economic recovery efforts, including stimulus packages, financial assistance programs, and initiatives to support struggling industries.

Figure 5 | Time series analysis of (a) temperature (°C), (b) rainfall amount (mm), and (c) max wind speed (km/h).

Overall, while there were similarities between 2020 and 2021 in terms of quarantine restrictions and reduced human activity, 2021 saw more targeted approaches and efforts towards recovery as vaccination efforts progressed and more understanding was gained about controlling the spread of COVID-19. In addition, many activities that were halted in 2020 resumed.

Figure 6 | Time line of temporal variation of Chl-a and turbidity from 2016 to 2021.
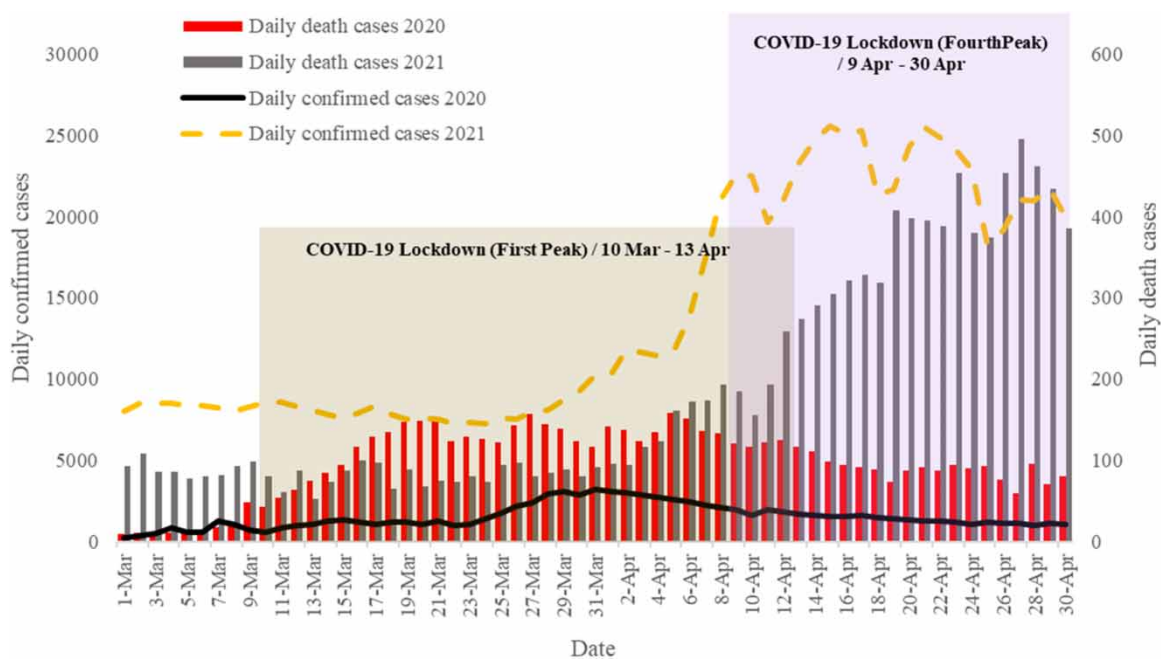
Figure 7 | Daily confirmed and death cases of COVID-19 in Iran in March and April of 2020 and 2021.

4. DISCUSSION

The current article investigates the effects of COVID-19 lockdowns on Chl-a and turbidity in the western part of Anzali Wetland and the cessation or reduction of pollutants entering the seas, lakes, and wetlands, as well as the reduction of human activities (fishing and boating). The time period selected in this study is from March 27 to April 27 from 2016 to 2021. This period was chosen for three reasons: (1) The weather and climate conditions are quite the same in the study region. (2) It embraces the first peak (March 10–April 13) and the fourth peak (April 9–30), which coincide with the COVID-19 lockdowns. (3) The free-cloud satellite imagery for the study region is available for this time interval.

Natural factors and human activities are two important factors that lead to changes in Chl-a concentration and turbidity (Sun *et al.* 2021). The human activities that affect the water quality of Anzali Wetland may include domestic sewage, adjacent residential regions, food industry effluents, and livestock that enter the rivers related to Anzali Wetland without any treatment. Also, the diversity of land use in the field and subsequently the entrance of organic and inorganic materials into the wetland are the most important reasons for reducing the water quality of Anzali Wetland and intensifying the nutritional process, with three main sources, namely, fertilizers used in agriculture, domestic sewage, and livestock waste (Fallah & Fakheran 2018). There are also natural factors including temperature, wind speed, rainfall, and number of sunny days.

In this study, the models suggested by Mishra & Mishra (2012) and Abirhire *et al.* (2020) were used to estimate the amount of Chl-a concentration and turbidity, respectively. Both models have shown good results in previous studies (Watanabe *et al.* 2015; Beck *et al.* 2016; Abirhire *et al.* 2020; Lai *et al.* 2021; Li *et al.* 2021; Muduli *et al.* 2021). Ergo, the Chl-a concentration, and turbidity were estimated in the desired period, and output maps were produced by ENVI and ArcGIS (Figures 2 and 3). As shown, it is observed that the Chl-a concentration in 2020 is lower than that in the previous years, while water turbidity has decreased significantly in 2020. However, the Chl-a concentration during the lockdown of 2021 has increased significantly compared with that of 2020 and reached 20.9 μg/L. The Chl-a concentration and turbidity were expected to decrease significantly due to COVID-19 lockdowns as a result of the reduced nutrient input from industrial effluents and agricultural activities.

According to Table 4, Chl-a and turbidity showed 26 and 16% decrease in 2020 (the first peak lockdown), respectively, compared to the average of 2016 to 2019. In 2021 (the fourth peak lockdown), water turbidity decreased by 1% compared to the average of 2016 to 2019, whereas the Chl-a concentration increased by 21%. Natural and physical factors such as water temperature and sunlight may increase Chl-a (Ganguly *et al.* 2013; Vardhan Kanuri *et al.* 2013; Muduli *et al.* 2021). The estimations of water turbidity and Chl-a in the study area were compared with the field-based measurements to check their accuracy. Based on Figure 4, the results reveal a significant relationship between the measured values with the ones estimated by Mishra and Mishra's model (2012) and Abirhire *et al.*'s model (2020).

The possible effects of natural factors on the two water quality parameters were investigated in Figure 5. The meteorological data of the study area included rainfall (rainy days and total monthly rainfall), temperature (daily air temperature, the minimum, maximum, and average monthly temperature), and wind speed. As illustrated in Figure 5, the average temperature in the period under study in 2021 has increased compared to the previous years. Given the relationship between air temperature and water temperature, it may be possible that as the air temperature rises, the water temperature also increases (Harvey *et al.* 2011). Increasing water temperature can affect the growth of Chl-a (Ganguly *et al.* 2013; Vardhan Kanuri *et al.* 2013). In addition, the low rainfall in April 2021 compared to the previous years reduced the likelihood of rivers entering and regenerating foam (Penning *et al.* 2013; Sun *et al.* 2021) and played a smaller role in turbidity changes than in the previous years. Furthermore, the sharp decline in human activities due to the COVID-19 lockdowns could be another possible factor in significantly reducing water turbidity in 2020. Agricultural runoff, domestic sewage, and industrial effluents were among these factors (Abedini *et al.* 2018; ALabdeh *et al.* 2020), many of which were reduced during the COVID-19 lockdowns. The possible reasons for the increase in Chl-a in April 2021 were also examined:

1. It is possible that human activities, such as agriculture and industrial activities, increased to compensate for the economic losses caused by restrictions and lockdowns from April 2020 to April 2021. With increasing agricultural and industrial activities, the nutrients introduced into the water increase and can affect Chl-a as well as increasing turbidity.
2. Anzali Wetland is one of the tourist centres in Iran. At the beginning of the Iranian New Year on 21 March 2021, travel increased and tourist centres increased their activities. This can be another possible factor affecting turbidity and Chl-a in the period under investigation.
3. The study of Chl-a and turbidity by satellite images in 2021 started only 10 days after the start of the fourth peak lockdown, whereas the studies were 21 days after the start of the first peak lockdown in 2020. In this context, the water body had more opportunity to revive itself.
4. Although the major benefit of investigating confirmed and death COVID-19 cases will become handy for healthcare systems (Niazkar & Niazkar 2020), this information can be further used to testify environmental findings. Based on Figure 7, it is indicated that quarantine practices were taken seriously by the people in

the first peak owing to the new arrival of the virus in Iran and maybe a great fear associated with the disease, which was unavoidably developed in public opinions. On the other hand, the numbers of positive and death COVID-19 cases are relatively more than those of the first peak, as shown in Figure 7. This increase occurred despite imposing a quarantine of the fourth peak in 2021. One of the possible reasons may be the lack of serious quarantine conditions conducted by people or government regulations. To be more precise, travels between cities because of the Iranian New Year increased in March 2021. Furthermore, factories attempted to somehow continue working in favour of compensating for economic losses even though their activities were restricted by quarantine regulations. As a result, the quarantine imposed in the fourth peak of the COVID-19 pandemic turns out to be a partial lockdown in practice. Therefore, human activities during the first peak were much fewer than those of the fourth peak. This evidence-based result deduced from Figure 7 is in agreement with variations of Chl-a and turbidity during the COVID-19 lockdowns. Moreover, Figures 6 and 7 clarify that the values of Chl-a and turbidity are lower in the first peak than those of the fourth peak because human activities in the former are much fewer than those in the fourth peak. Thus, reduced human activities due to the COVID-19 lockdowns are one of the vital factors, which may be responsible for the significant reduction of Chl-a concentrations and turbidity in 2020 and 2021.

One of the main limitations of this study was the inability to sample from the wetland due to the lockdown. This study is limited to only two water quality parameters: Chl-a and turbidity. However, other important parameters such as pH, DO, BOD, and COD exist, which should be evaluated for effective water quality management. Due to traffic restrictions caused by the COVID-19 pandemic, sampling of phosphorus and nitrogen parameters onsite was not possible in this research. It is recommended that these aspects be investigated in future studies. It is also suggested that, if possible, future studies investigate changes in land use during the quarantine period and articulate their impact on water quality.

Other studies have been conducted in various parts of the world, and their results, like this research, indicate that the constraints related to COVID-19 have led to an improvement in water quality. Cheval et al. (2020) reported that during the citywide COVID-19 lockdown in the spring of 2020, Venice witnessed a significant improvement in water quality due to reduced water transport and tourist activities. Similarly, Germany and Austria observed a decrease in water consumption. The authors emphasized the effectiveness of monitoring SARS-CoV-2 RNA in sewage waters as a tool for surveillance of coronavirus spread. They also highlighted the negative impact of the pandemic on water bodies, noting numerous reports of significant harm caused by medical and personal hygiene products littering the shores in various regions, including Hong Kong and Canada. Rume & Islam (2020) also noted in their research that the pandemic led to a decrease in water contamination across various countries. However, it also resulted in increased amounts of medical waste, disinfectants, and untreated personal protective equipment, all of which ultimately impacted the quality of water bodies. Rupani et al. (2020) reaffirmed the positive impact of the COVID-19 pandemic on the water quality of the Ganga River, which showed significant improvement. Reductions in water pollution were evident in Wuhan (China), Italy, France, Spain, and Los Angeles (USA). Yusoff et al. (2021) evaluated the positive and negative effects of the pandemic on aquatic organisms. The COVID-19 quarantine resulted in improved water quality and biodiversity. It also led to a reduction in the concentration of macroplastics, Chl-a, phytoplankton, and nitrogen in the coastal area of India.

5. CONCLUSIONS

The current study investigates turbidity and Chl-a concentration in the western part of Anzali Wetland from 27 March to 27 April from 2016 to 2021 using Sentinel 2/MSI satellite images. Also, efforts were made to assess impacts of the COVID-19 lockdowns on turbidity and Chl-a concentration of the study area. Satellite imagery showed a significant difference between 2020 and 2021 for turbidity and Chl-a. Comparing the estimated results in 2020 with the measured results of the previous years indicated 26 and 16% decreases in the amount of Chl-a and turbidity, respectively. Furthermore, 1% decrease in turbidity and 21% increase in the concentration of Chl-a were observed compared to the average amounts measured between 2016 and 2019. Natural factors, such as temperature and rainfall, were also influential in controlling the water quality condition. The increase in water temperature increased the probability of increasing the Chl-a concentration. On the other hand, the rainfall decreased in April 2021 compared to that of the previous years. The rainfall variation left a slight effect on turbidity changes. In addition to the low rainfall, the reduction of Chl-a and turbidity in 2020 could be attributed to a significant reduction in human activities and less discharge of effluents because Anzali Wetland is very much

affected by anthropogenic factors due to its proximity to urban regions and agricultural lands. On the other hand, the possible reasons for the increase in Chl-a and turbidity in 2021 were the increase in human activities (factories, agriculture, domestic sewage) and also the increase in tourism activities due to the beginning of the new year (before the start of the fourth peak lockdown). It is stipulated that the lockdown that restricted human activities, like the one imposed in the first peak of COVID-19 in 2020 in Iran, would significantly reduce the concentration of Chl-a and turbidity. Finally, factors affecting Chl-a and turbidity are various and complex, while the extent to which human activities affect the concentration of Chl-a and turbidity in the western part of Anzali Wetland still requires further research.

DATA AVAILABILITY STATEMENT

Data cannot be made publicly available; readers should contact the corresponding author for details.

CONFLICT OF INTEREST

The authors declare there is no conflict.

REFERENCES

Abedini, A., Mirzajani, A. R. & Fallahi, M. 2018 Physicochemical conditions and trophic levels of the Anzali wetland. *Iranian Scientific Fisheries Journal* **26**(6), 113–123. Available from: http://isfj.ir/article-1-1858-en.html. (In Persian).

Abirhire, O., Davies, J.-M., Guo, X. & Hudson, J. 2020 Understanding the factors associated with long-term reconstructed turbidity in Lake Diefenbaker from Landsat-imagery. *Science of the Total Environment* **724**, 138222. https://doi.org/10.1016/j.scitotenv.2020.138222.

Aghsaei, H., Mobarghaee Dinan, N., Moridi, A., Asadolahi, Z., Delavar, M., Fohrer, N. & Wagner, P. D. 2020 Effects of dynamic land use/land cover change on water resources and sediment yield in the Anzali wetland catchment, Gilan, Iran. *Science of the Total Environment* **712**, 136449. https://doi.org/10.1016/j.scitotenv.2019.136449.

ALabdeh, D., Omidvar, B., Karbassi, A. & Sarang, A. 2020 Study of water quality parameters of Anzali wetland using a proposed method of combining Blind Kriging and Linear Regression. *Wetland Ecobiology* **12**(3), 55–70. http://jweb.iauahvaz.ac.ir/article-1-885-en.html. (In Persian).

Aman, M. A., Salman, M. S. & Yunus, A. P. 2020 COVID-19 and its impact on environment: Improved pollution levels during the lockdown period – A case from Ahmedabad, India. *Remote Sensing Applications: Society and Environment* **20**, 100382. https://doi.org/10.1016/j.rsase.2020.100382.

Avtar, R., Kumar, P., Supe, H., Jie, D., Sahu, N., Mishra, B. K. & Yunus, A. P. 2020 Did the COVID-19 lockdown-induced hydrological residence time intensify the primary productivity in lakes? Observational results based on satellite remote sensing. *Water* **12**(9), 2573. https://doi.org/10.3390/w12092573.

Baughman, C. A., Jones, B. M., Bartz, K. K., Young, D. B. & Zimmerman, C. E. 2015 Reconstructing turbidity in a glacially influenced lake using the Landsat TM and ETM+ surface reflectance climate data record archive, lake Clark, Alaska. *Remote Sensing* **7**(10), 13692–13710. https://doi.org/10.3390/rs71013692.

Beck, R., Zhan, S., Liu, H., Tong, S., Yang, B., Xu, M., Ye, Z., Huang, Y., Shu, S., Wu, Q., Wang, S., Berling, K., Murray, A., Emery, E., Reif, M., Harwood, J., Young, J., Nietch, C., Macke, D., Martin, M., Stillings, G., Stump, R. & Su, H. 2016 Comparison of satellite reflectance algorithms for estimating chlorophyll-a in a temperate reservoir using coincident hyperspectral aircraft imagery and dense coincident surface observations. *Remote Sensing of Environment* **178**, 15–30. https://doi.org/10.1016/j.rse.2016.03.002.

Bhadra, A., Mukherjee, A. & Sarkar, K. 2021 Impact of population density on COVID-19 infected and mortality rate in India. *Modeling Earth Systems and Environment* **7**(1), 623–629. https://doi.org/10.1007/s40808-020-00984-7.

Buma, W. G. & Lee, S.-I. 2020 Evaluation of Sentinel-2 and Landsat 8 images for estimating chlorophyll-a concentrations in Lake Chad, Africa. *Remote Sensing* **12**(15), 2437. https://doi.org/10.3390/rs12152437.

Cherif, E. K., Vodopivec, M., Mejjad, N., Esteves da Silva, J. C. G., Simonovič, S. & Boulaassal, H. 2020 COVID-19 pandemic consequences on coastal water quality using WST Sentinel-3 data: Case of Tangier, Morocco. *Water* **12**(9), 2638. https://doi.org/10.3390/w12092638.

Cheval, S., Mihai Adamescu, C., Georgiadis, T., Herrnegger, M., Piticar, A. & Legates, D. R. 2020 Observed and potential impacts of the COVID-19 pandemic on the environment. *International Journal of Environmental Research and Public Health* **17**(11), 4140. Available from: https://www.mdpi.com/1660-4601/17/11/4140.

Fallah, M. & Zamani-Ahmadmahmoodi, R. 2017 Assessment of water quality in Iran's Anzali Wetland, using qualitative indices from 1985, 2007, and 2014. *Wetlands Ecology and Management* **25**(5), 597–605. https://doi.org/10.1007/s11273-017-9538-y.

Fallah, M. & Fakheran, S. 2018 Assessment of the water quality of the Anzali International Wetland using Qualitative Indices. *Journal of Water and Sustainable Development* **4**(2), 23–30. doi:10.22067/JWSD.V4I2.61307.

Ganguly, D., Robin, R. S., Vardhan, K. V., Muduli, P. R., Abhilash, K. R., Patra, S. & Subramanian, B. R. 2013 Variable response of two tropical phytoplankton species at different salinity and nutrient condition. *Journal of Experimental Marine Biology and Ecology* **440**, 244–249. https://doi.org/10.1016/j.jembe.2013.01.008.

Garg, V., Aggarwal, S. P. & Chauhan, P. 2020 Changes in turbidity along Ganga River using Sentinel-2 satellite data during lockdown associated with COVID-19. *Geomatics, Natural Hazards and Risk* **11**(1), 1175–1195. https://doi.org/10.1080/19475705.2020.1782482.

Gholizadeh, M. H., Melesse, A. M. & Reddi, L. 2016 A comprehensive review on water quality parameters estimation using remote sensing techniques. *Sensors* **16**(8), 1298. https://doi.org/10.3390/s16081298.

Goodarzi, M. R., Pooladi, R. & Niazkar, M. 2022a Evaluation of satellite-based and reanalysis precipitation datasets with Gauge-observed data over Haraz-Gharehsoo Basin, Iran. *Sustainability* **14**(20), 13051. Available from: https://www.mdpi.com/2071-1050/14/20/13051.

Goodarzi, M. R., Sabaghzadeh, M. & Mokhtari, M. H. 2022b Impacts of aspect on snow characteristics using remote sensing from 2000 to 2020 in Ajichai-Iran. *Cold Regions Science and Technology* **204**, 103682. https://doi.org/https://doi.org/10.1016/j.coldregions.2022.103682.

Goodarzi, M. R., Niknam, A. R. R., Rahmati, S. H. & Attar, N. F. 2023 Assessing land use changes' effect on river water quality in the Dez Basin using land change modeler. *Environmental Monitoring and Assessment* **195**(6), 774. https://doi.org/10.1007/s10661-023-11265-y.

Harvey, R., Lye, L., Khan, A. & Paterson, R. 2011 The influence of air temperature on water temperature and the concentration of dissolved oxygen in Newfoundland rivers. *Canadian Water Resources Journal/Revue Canadienne des Ressources Hydriques* **36**(2), 171–192. https://doi.org/10.4296/cwrj3602849.

Hicks, B. J., Stichbury, G. A., Brabyn, L. K., Allan, M. G. & Ashraf, S. 2013 Hindcasting water clarity from Landsat satellite images of unmonitored shallow lakes in the Waikato region, New Zealand. *Environmental Monitoring and Assessment* **185**(9), 7245–7261. https://doi.org/10.1007/s10661-013-3098-2.

Hosseinjani, A., Ahmadnezhad, M. & Sayyad Bourani, M. 2019 Introduction to the flora, life forms and chorology of the western region of Anzali wetland (Abkenar wetland). *Ecology and Water Resources* **3**(1), 49–56. Available from: https://ewrj.areeo.ac.ir/article_121107.html?lang=en. (In Persian).

Khan, R., Saxena, A., Shukla, S., Sekar, S. & Goel, P. 2021 Effect of COVID-19 lockdown on the water quality index of River Gomti, India, with potential hazard of faecal-oral transmission. *Environmental Science and Pollution Research* **28**(25), 33021–33029. https://doi.org/10.1007/s11356-021-13096-1

Lai, Y., Zhang, J., Song, Y. & Gong, Z. 2021 Retrieval and evaluation of chlorophyll-a concentration in reservoirs with main water supply function in Beijing, China, based on Landsat Satellite images. *International Journal of Environmental Research and Public Health* **18**, 9. https://doi.org/10.3390/ijerph18094419.

Li, S., Song, K., Wang, S., Liu, G., Wen, Z., Shang, Y., Lyu, L., Chen, F., Xu, S., Tao, H., Du, Y., Fang, C. & Mu, G. 2021 Quantification of chlorophyll-a in typical lakes across China using Sentinel-2 MSI imagery with machine learning algorithm. *Science of the Total Environment* **778**, 146271. https://doi.org/10.1016/j.scitotenv.2021.146271.

Mahdavifard, M., Valizadeh Kamran, K. & Atazadeh, E. 2020 Estimation of chlorophyll-a concentration using ground data and Sentinel-2 and Landsat-8 Satellite images processing (case study: Tiab Estuary). *Journal of RS and GIS for Natural Resources* **11**. Available from: http://girs.iaubushehr.ac.ir/article_672377_en.html. (In Persian).

Mansouri Daneshvar, M. R., Ebrahimi, M., Sadeghi, A. & Mahmoudzadeh, A. 2022 Climate effects on the COVID-19 outbreak: A comparative analysis between the UAE and Switzerland. *Modeling Earth Systems and Environment* **8**(1), 469–482. https://doi.org/10.1007/s40808-021-01110-x.

Martins, V. S., Kaleita, A., Barbosa, C. C. F., Fassoni-Andrade, A. C., Lobo, F. d. L. & Novo, E. M. L. M. 2019 Remote sensing of large reservoir in the drought years: Implications on surface water change and turbidity variability of Sobradinho reservoir (Northeast Brazil). *Remote Sensing Applications: Society and Environment* **13**, 275–288. https://doi.org/10.1016/j.rsase.2018.11.006.

Masocha, M., Dube, T., Nhiwatiwa, T. & Choruma, D. 2018 Testing utility of Landsat 8 for remote assessment of water quality in two subtropical African reservoirs with contrasting trophic states. *Geocarto International* **33**(7), 667–680. https://doi.org/10.1080/10106049.2017.1289561.

Mishra, S. & Mishra, D. R. 2012 Normalized difference chlorophyll index: A novel model for remote estimation of chlorophyll-a concentration in turbid productive waters. *Remote Sensing of Environment* **117**, 394–406.

Muduli, P. R., Kumar, A., Kanuri, V. V., Mishra, D. R., Acharya, P., Saha, R., Biswas, M. K., Vidyarthi, A. K. & Sudhakar, A. 2021 Water quality assessment of the Ganges River during COVID-19 lockdown. *International Journal of Environmental Science and Technology* **18**(6), 1645–1652. https://doi.org/10.1007/s13762-021-03245-x.

Najah, A., Teo, F. Y., Chow, M. F., Huang, Y. F., Latif, S. D., Abdullah, S., Ismail, M. & El-Shafie, A. 2021 Surface water quality status and prediction during movement control operation order under COVID-19 pandemic: Case studies in Malaysia', International. *Journal of Environmental Science and Technology* **18**(4), 1009–1018. https://doi.org/10.1007/s13762-021-03139-y.

Nas, B., Ekercin, S., Karabörk, H., Berktay, A. & Mulla, D. 2010 An application of Landsat-5TM image data for water quality mapping in Lake Beysehir, Turkey. *Water, Air, & Soil Pollution* **212**, 183–197. http://dx.doi.org/10.1007/s11270-010-0331-2.

Niazkar, H. R. & Niazkar, M. 2020 COVID-19 international outbreak and the need for a suitable estimation model: A second-order polynomial equation with constant coefficients based on imported infected cases seems inadequate. *Asian Pacific Journal of Tropical Medicine* **13**, 4. http://dx.doi.org/10.4103/1995-7645.280234.

Niazkar, M., Eryılmaz Türkkan, G., Niazkar, H. R. & Türkkan, Y. A. 2020 Assessment of three mathematical prediction models for forecasting the COVID-19 outbreak in Iran and Turkey. *Computational and Mathematical Methods in Medicine* **2020**, 7056285. http://dx.doi.org/10.1155/2020/7056285.

Niknam, A. R. R., Sabaghzadeh, M., Barzkar, A. & Shishebori, D. 2024 Comparing ARIMA and various deep learning models for long-term water quality index forecasting in Dez River, Iran. *Environmental Science and Pollution Research* https://doi.org/10.1007/s11356-024-32228-x.

Niroumand-Jadidi, M., Bovolo, F., Bruzzone, L. & Gege, P. 2020 Physics-based bathymetry and water quality retrieval using planetScope imagery: impacts of 2020 COVID-19 lockdown and 2019 extreme flood in the Venice Lagoon. *Remote Sensing* **12**(15), 2381. https://doi.org/10.3390/rs12152381.

Patel, P. P., Mondal, S. & Ghosh, K. G. 2020 Some respite for India's dirtiest river? Examining the Yamuna's water quality at Delhi during the COVID-19 lockdown period. *Science of the Total Environment* **744**, 140851. https://doi.org/10.1016/j.scitotenv.2020.140851.

Penning, W. E., Genseberger, M., Uittenbogaard, R. E. & Cornelisse, J. C. 2013 Quantifying measures to limit wind-driven resuspension of sediments for improvement of the ecological quality in some shallow Dutch lakes. *Hydrobiologia* **710**(1), 279–295. https://doi.org/10.1007/s10750-012-1026-z.

Rahman, M. R., Islam, A. H. M. H. & Islam, M. N. 2021 Geospatial modelling on the spread and dynamics of 154 day outbreak of the novel coronavirus (COVID-19) pandemic in Bangladesh towards vulnerability zoning and management approaches. *Modeling Earth Systems and Environment* **7**(3), 2059–2087. https://doi.org/10.1007/s40808-020-00962-z.

Ritchie, J. C., Zimba, P. V. & Everitt, J. H. 2003 Remote sensing techniques to assess water quality. *Photogrammetric Engineering & Remote Sensing* **69**(6), 695–704. https://doi.org/10.14358/PERS.69.6.695.

Roy, S., Bhunia, G. S. & Shit, P. K. 2021 Spatial prediction of COVID-19 epidemic using ARIMA techniques in India. *Modeling Earth Systems and Environment* **7**(2), 1385–1391. https://doi.org/10.1007/s40808-020-00890-y.

Rume, T. & Islam, S. M. D.-U. 2020 Environmental effects of COVID-19 pandemic and potential strategies of sustainability. *Heliyon* **6**(9). https://doi.org/10.1016/j.heliyon.2020.e04965.

Rupani, P. F., Nilashi, M., Abumalloh, R. A., Asadi, S., Samad, S. & Wang, S. 2020 Coronavirus pandemic (COVID-19) and its natural environmental impacts. *International Journal of Environmental Science and Technology* **17**(11), 4655–4666. https://doi.org/10.1007/s13762-020-02910-x.

Sun, X., Liu, J., Wang, J., Tian, L., Zhou, Q. & Li, J. 2021 Integrated monitoring of lakes' turbidity in Wuhan, China during the COVID-19 epidemic using multi-sensor satellite observations. *International Journal of Digital Earth* **14**(4), 443–463. https://doi.org/10.1080/17538947.2020.1868584.

Tokatlı, C. & Varol, M. 2021 Impact of the COVID-19 lockdown period on surface water quality in the Meriç-Ergene River Basin, Northwest Turkey. *Environmental Research* **197**, 111051. https://doi.org/10.1016/j.envres.2021.111051.

Vardhan Kanuri, V., Muduli, V., Robin, P. R., Charan Kumar, R. S., Lovaraju, B., Ganguly, A., Patra, D., Nageswara Rao, S., Raman, G., and Subramanian, A. V. & R, B. 2013 Plankton metabolic processes and its significance on dissolved organic carbon pool in a tropical brackish water lagoon. *Continental Shelf Research* **61–62**, 52–61. https://doi.org/10.1016/j.csr.2013.04.006.

Venter, Z. S., Aunan, K., Chowdhury, S. & Lelieveld, J. 2020 COVID-19 lockdowns cause global air pollution declines. *Proceedings of the National Academy of Sciences* **117**(32), 18984. https://doi.org/10.1073/pnas.2006853117.

Wang, F., Han, L., Kung, H. T. & Van Arsdale, R. B. 2006 Applications of Landsat-5 TM imagery in assessing and mapping water quality in Reelfoot Lake, Tennessee. *International Journal of Remote Sensing* **27**(23), 5269–5283. https://doi.org/10.1080/01431160500191704.

Watanabe, F. S. Y., Alcântara, E., Rodrigues, T. W. P., Imai, N. N., Barbosa, C. C. F. & Rotta, L. H. d. S. 2015 Estimation of chlorophyll-a concentration and the Trophic State of the Barra Bonita Hydroelectric Reservoir using OLI/Landsat-8 images. *International Journal of Environmental Research and Public Health* **12**(9), 10391–10417. https://doi.org/10.3390/ijerph120910391.

Xing, Z., Chua, L. H. C., Miao, H., Imberger, J. & Yang, P. 2018 Wind shielding impacts on water quality in an urban reservoir. *Water Resources Management* **32**(11), 3549–3561. Available from: https://link.springer.com/article/10.1007/s11269-018-1980-y.

Xu, H., Xu, G., Wen, X., Hu, X. & Wang, Y. 2021 Lockdown effects on total suspended solids concentrations in the Lower Min River (China) during COVID-19 using time-series remote sensing images. *International Journal of Applied Earth Observation and Geoinformation* **98**, 102301. https://doi.org/10.1016/j.jag.2021.102301.

Yunus, A. P., Masago, Y. & Hijioka, Y. 2020 COVID-19 and surface water quality: Improved lake water quality during the lockdown. *Science of the Total Environment* **731**, 139012. https://doi.org/10.1016/j.scitotenv.2020.139012.

Yusoff, F. M., Abdullah, A. F., Aris, A. Z. & Umi, W. A. D. 2021 Impacts of COVID-19 on the aquatic environment and implications on aquatic food production. *Sustainability* **13**(20), 11281. Available from: https://www.mdpi.com/2071-1050/13/20/11281.